AD-A141 741 SINGLE CRYSTAL GROWTH OF FERROELECTRIC TUNGSTEN BRONZE 1/1
COMPOSITIONS FOR S..(U) ROCKWELL INTERNATIONAL THOUSAND
OAKS CA SCIENCE CENTER R R NEURGAONKAR FEB 84
UNCLASSIFIED SC5348.1FR AFOSR-TR-84-0435 F/G 20/2 NL

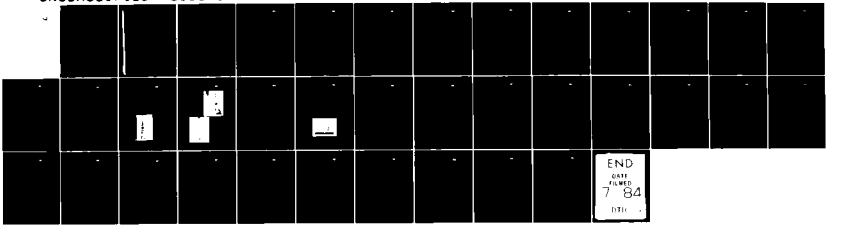

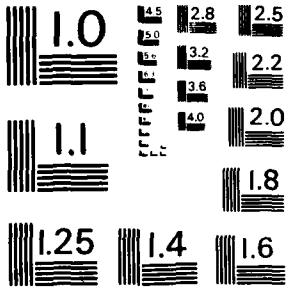

MICROCOPY RESOLUTION TEST CHART
NATIONAL BUREAU OF STANDARDS - 1963 - A

AFOSR TR- 84-0435

6

SC5346.1FR

SINGLE CRYSTAL GROWTH OF FERROELECTRIC TUNGSTEN BRONZE COMPOSITIONS FOR SAW APPLICATIONS

(12)

FINAL REPORT
FOR PERIOD 07/26/82 THROUGH 12/31/83

FEBRUARY 1984

Name of Contractor:	Rockwell International Corporation
Effective Date of Contract:	July 26, 1982
Contract Expiration Date:	December 31, 1983
Amount of Contract Dollars:	$85,000
Contract Number:	F49620-82-C-0078
Principal Investigator:	Dr. R.R. Neurgaonkar (805) 498-4545, Ext. 109

Sponsored by

Air Force Office of Scientific Research
Directorate of Electronic and Material Sciences
Building 410
Bolling AFB, DC 20332

Research sponsored by the Air Force Office of Scientific Research (AFSC), under Contract F49620-82-C-0078. The United States Government is authorized to reproduce and distribute reprints for governmental purposes notwithstanding any copyright notation hereon.

The views and conclusions contained in this document are those of the authors and should not be interpreted as necessarily representing the official policies or endorsements, either expressed or implied, of the Air Force Office of Scientific Research or the U.S. Government.

Approved for public release; distribution unlimited

UNCLASSIFIED
SECURITY CLASSIFICATION OF THIS PAGE

AD-A141741

REPORT DOCUMENTATION PAGE

1a. REPORT SECURITY CLASSIFICATION Unclassified	1b. RESTRICTIVE MARKINGS
2a. SECURITY CLASSIFICATION AUTHORITY	3. DISTRIBUTION/AVAILABILITY OF REPORT Approved for public release; distribution unlimited.
2b. DECLASSIFICATION/DOWNGRADING SCHEDULE	
4. PERFORMING ORGANIZATION REPORT NUMBER(S) SC5346.1FR	5. MONITORING ORGANIZATION REPORT NUMBER(S) AFOSR-TR- 84-0435
6a. NAME OF PERFORMING ORGANIZATION Rockwell International Science Center 6b. OFFICE SYMBOL (If applicable)	7a. NAME OF MONITORING ORGANIZATION AFOSR/NE
6c. ADDRESS (City, State and ZIP Code) 1049 Camino Dos Rios Thousand Oaks, California 91360	7b. ADDRESS (City, State and ZIP Code) Bolling AFB, DC.
8a. NAME OF FUNDING/SPONSORING ORGANIZATION Air Force Office of Scientific Research 8b. OFFICE SYMBOL (If applicable)	9. PROCUREMENT INSTRUMENT IDENTIFICATION NUMBER Contract No. F49620-82-C-0078
8c. ADDRESS (City, State and ZIP Code) Building 410 Bolling AFB, DC 20332	10. SOURCE OF FUNDING NOS. PROGRAM ELEMENT NO. 61102F; PROJECT NO. 2306; TASK NO. B1; WORK UNIT NO.
11. TITLE (Include Security Classification) SINGLE CRYSTAL GROWTH OF FERROELECTRIC TUNGSTEN BRONZE COMPOSITIONS FOR SAW APPLICATIONS (U)	
12. PERSONAL AUTHOR(S) Neurgaonkar, Ratnakar R.	
13a. TYPE OF REPORT Final Technical Report 13b. TIME COVERED FROM 07/26/82 TO 12/31/83	14. DATE OF REPORT (Yr., Mo., Day) FEBRUARY 1984 15. PAGE COUNT 32
16. SUPPLEMENTARY NOTATION	
17. COSATI CODES FIELD / GROUP / SUB. GR.	18. SUBJECT TERMS (Continue on reverse if necessary and identify by block number)

19. ABSTRACT (Continue on reverse if necessary and identify by block number)

Ferroelectric tungsten bronze single crystals (e.g. $K_3Li_2Nb_5O_{15}$, $Ba_{2-x}Sr_xK_{1-y}Na_yNb_5O_{15}$ and $Pb_{1-x}Ba_xNb_2O_6$) were grown by the Czochralski technique. The crystals belong to the tetragonal point group 4mm with spontaneous polarization parallel to the 'c' axis. Room temperature dielectric and piezoelectric measurements indicated that the k_{15} and d_{15} coefficients are significantly larger for these bigger unit cell bronzes as compared to the smaller unit cell bronzes, e.g. SBN, SKN, etc. The results of this study indicate that since the piezoelectric properties of these crystals are better than SBN, it is expected that these composition crystals should show better acoustical properties. As reported earlier, SBN crystals are known to possess excellent acoustical properties and are useful for device application. Hence, this opens up further new interest in this family of crystals for potential use in SAW device applications.

20. DISTRIBUTION/AVAILABILITY OF ABSTRACT UNCLASSIFIED/UNLIMITED ☒ SAME AS RPT. ☐ DTIC USERS ☐	21. ABSTRACT SECURITY CLASSIFICATION Unclassified
22a. NAME OF RESPONSIBLE INDIVIDUAL Col. Harry Winsor and Dr. Kevin Melloy	22b. TELEPHONE NUMBER (Include Area Code) 202-693-0013 22c. OFFICE SYMBOL

DD FORM 1473, 83 APR EDITION OF 1 JAN 73 IS OBSOLETE.

UNCLASSIFIED
SECURITY CLASSIFICATION OF THIS PAGE

TABLE OF CONTENTS

LIST OF FIGURES

LIST OF TABLES

1.0 INTRODUCTION

The present work on ferroelectric tungsten bronze crystals for the acoustical surface wave project was initiated with the specific objective of developing a superior material for SAW device studies. These SAW devices are very important and are commonly used to solve problems in the technological areas of bandpass filters, resonators, oscillators, and discriminators. All of these devices are, however, limited in their performance by SAW materials availability. A large number of ferroelectric crystals have been grown and characterized, and many of these have properties that are extremely attractive for SAW device applications. In particular, many of the ferroelectrics have high surface acoustic wave velocity and possess temperature compensated orientations. However, only a few ferroelectrics such as $LiNbO_3$, $LiTaO_3$, and α-SiO_2 have found wide application in the acoustical area. Other ferroelectric materials which exhibit much higher piezoelectric, elastic and acoustical properties, as well as temperature compensated orientations (e.g., $Pb_2KNb_5O_{15}$, $Ba_2NaNb_5O_{15}$), have not been fully exploited on a practical basis because of difficulties in growing large and good quality single crystals.

The present research and development work was undertaken with the goal to identify and establish suitable tungsten bronze ferroelectric crystals which possess high surface acoustic wave electromechanical coupling constants (K^2) with a sufficiently low temperature coefficient of SAW velocity. The recent success at our laboratory in growing large single crystals of SBN:60, SBN:50, BSKNN, KLN and PBN could represent a major breakthrough in new materials development for potential SAW device applications. We recently demonstrated that both SBN:60 and SBN:50 composition crystals exhibit high SAW electromechanical coupling constants, e.g., 180×10^{-4} and 230×10^{-4}, respectively. These constants were measured for (001)-plates propagating along the (100) direction. These values are smaller than the best known piezoelectric Y-Z cut $LiNbO_3$ crystal (480×10^{-4}), but they are similar to the best known piezoelectric tungsten bronze $Pb_2KNb_5O_{15}$ crystal (188×10^{-4}). Furthermore, both orthorhombic $Pb_2KNb_5O_{15}$ and tetragonal SBN:60 and SBN:50 crystals exhibit

temperature compensated orientations, indicating that there is a possibility of another tetragonal bronze crystal which may show suitable piezoelectric and acoustical characteristics.

The results of the present investigations indicate that the bigger unit cell tetragonal tungsten bronze crystals such as KLN, BSKNN and PBN show better ferroelectric and piezoelectric properties (e.g., d_{15}, k_{15}, k_{33}, elastic and other) as compared to the smaller unit cell bronze crystals such as SBN:60 and SBN:50. Although the growth of the bigger unit cell bronze crystals has been found to be difficult, the size of current crystals is sufficient to conduct all of the necessary acoustical and piezoelectric characterization. The goals of the present work were as follows:

- Establish crystal chemistry control for different bronze crystals to optimize the piezoelectric and acoustical properties.

- Establish the Czochralski bulk crystal growth technique for bigger unit cell bronze compositions, e.g., KLN, BSKNN and PBN.

- Determine the piezoelectric, piezoelastic and acoustical properties of these bronze compositions.

- Based on these results, establish the optimum bronze compositions with high electromechanical coupling constants (K^2) and sufficiently low temperature coefficient of SAW velocity.

2.0 MATERIALS DEVELOPMENT

2.1 Tungsten Bronze Family

The aim of the present research work has been to establish a suitable class of tungsten bronze materials with good SAW electromechanical coupling constants K^2 and low temperature coefficient SAW velocities suitable for further surface acoustic wave device development.

In seeking new materials which have high dielectric constants, high coupling constants or possibly high electro-optic coefficients, it is important to look for families which originate from high prototype symmetry with the possibility for low temperature ferroelectric:ferroelastic phase transitions. In this regard, the tungsten bronze structural family is potentially important and hence it could be used as principal host material. The bronze compositions can be represented by general formulae $(A_1)_4(A_2)_2(B)_{10}O_{30}$ and $(A_1)_4(A_2)_2C_4(B)_{10}O_{30}$, A_1, A_2, C and B are 15-, 12-, 9- and 6-fold coordinated sites in the structure (Fig. 1). Table 1 shows the structural transition and ferroic behavior of this family when different ions are substituted in the various crystallographic positions. This family embraces some 120 or more known compounds and various solid solution systems, and hence there is a good possibility of obtaining suitable compositions of the desired properties. Within this very extensive group, several members have high Curie temperatures, and have high dielectric, piezoelectric, electro-optic and pyroelectric coefficients.[1-12] According to work by Neurgaonkar et al.,[2,13] some of the bronze compositions such as $Sr_{1-x}Ba_xNb_2O_6$ possess temperature-compensated orientations and are potentially important for surface acoustic wave (SAW) device applications.

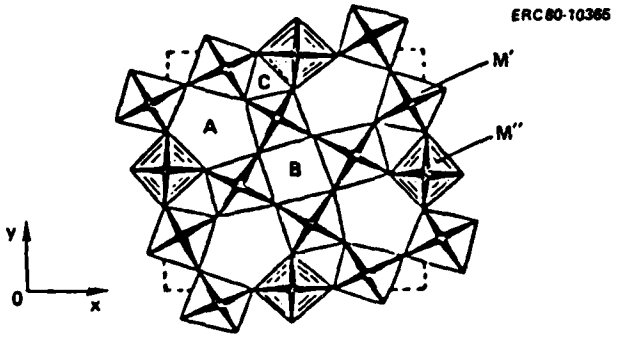

Fig. 1
Crystal structures.

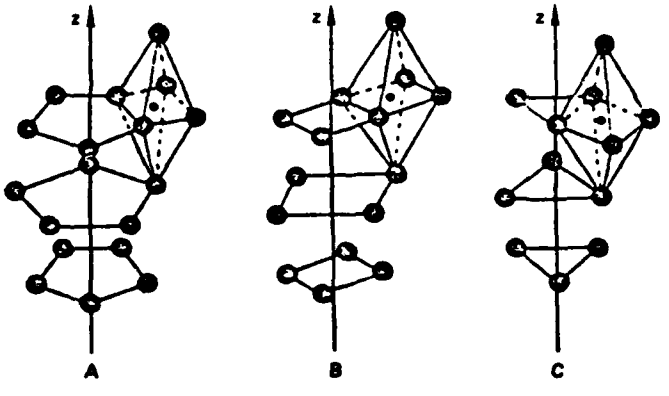

The composition $Sr_{0.61}Ba_{0.39}Nb_2O_6$ in particular shows an excellent SAW coupling coefficient K^2 of 188×10^{-4} and a low temperature coefficient of SAW velocity at room temperature.[2] However, modelling studies under DARPA Contract[13] have shown that these qualities can be substantially improved by selecting other bronze compositions with higher Curie temperatures than SBN. In particular, the compositions $K_3Li_2Nb_5O_{15}$ (KLN), $Pb_{1-x}Ba_xNb_2P_6$ (PBN), and $Ba_{2-x}Sr_xK_{1-y}Na_yNb_5O_5$ (BSKNN), are similar to SBN but have much higher Curie temperatures and better piezoelectric properties. The present work on the growth and characterization of these materials is given in the following sections.

Table 1

The Structural Sequences and Ferroelectric Behavior of the Various Tungsten Bronze Phases

Compound	No. of Transitions	Transitions Sequences			
$K_3Nb_5O_{13}F_2$	None	4/mmm Paraelectric/Paraelastic			
$Sr_2KNb_5O_{15}$ $K_3Li_2Nb_5O_{15}$ $Ba_6Ti_2Nb_8O_{30}$	One	4 mm Ferroelectric → Ferroelastic	4/mmm Paraelectric/Paraelastic		
$Sr_2K_{0.5}Li_{0.5}Nb_5O_{15}$	One	mm4 Ferroelastic → Ferroelastic	4/mmm Paraelastic Paraelastic		
$Pb_2KNb_5O_{15}$	One	mm2 Ferroelectric → Ferroelastic	4/mmm Paraelastic Paraelastic		
$Sr_2KTa_5O_{15}$	Two	mm2 Ferroelastic → Ferroelastic	mmm Paraelastic → Ferroelastic	4/mmm Paraelectric Paraelastic	
$Pb_{2.7}K_{0.56}Nb_{0.91}Ta_{4.15}O_{15}$	Two	mm2 Ferroelectric → Ferroelastic	mmm Paraelectric → Ferroelastic	4/mmm Paraelectric Paraelastic	
$Ba_2NaNb_5O_{15}$	Three	4mm Ferroelectric → Paraelastic	mm2 Ferroelectric → Ferroelastic	4 mm Ferroelectric → Ferroelastic	4/mmm Paraelectric → Paraelastic
$Ba_{2.14}Li_{0.71}Nb_{2.5}Ta_{2.5}O_{15}$	Three	4mm Antiferroelectric → Ferroelastic	mm2 Ferroelectric → Ferroelastic	4mm Paraelectric → Paraelastic	4/mmm Paraelectric → Paraelastic

2.2 Bulk Single Crystal Growth of T.B. Family Crystals

2.2.1 Growth Problems

The materials used for growth were specpure K_2CO_3, Li_2CO_3, Na_2CO_3, $BaCO_3$, $SrCO_3$, PbO, and Nb_2O_5. Table 2 summarizes the compositions of the

Table 2

Czochralski Growth Data for Tetragonal Tungsten Bronze Compositions

Composition	Growth Temperature (°C)	Growth Direction	Growth Habit	Crystal Diameter (cm)	Remarks
$Sr_{0.6}Ba_{0.4}Nb_2O_6$	1510	(001)	Cylindrical	~3.0	Crack-free and excellent quality
$Ba_{2-x}Sr_xK_{1-y}Na_yNb_5O_{15}$	1480	(001)	Square	~0.8 to 1.0	Crack-free and good quality
$K_3Li_2Nb_5O_{16}$*	1050	(001)	Square	0.3 to 0.5	Cracks
		(100)	Square	0.5 to 0.8	Crack-free, reasonable quality
		(110)	Square	0.5 to 0.8	Crack-free, reasonable quality
$K_3Li_2Nb_{5-x}Ta_xO_{15}$	1000-1250	(001) (110)	Square	0.5 to 1.0	Reasonable quality with excellent properties
$Pb_{0.33}Ba_{0.70}Nb_{1.987}O_6$**	~1350	(001)		0.8 to 1.0	Few cracks, but excellent properties

*Difficult to grow
**Grown at Penn State, difficult to grow.

individual crystals and their growth conditions. The starting materials were weighed out according to stoichiometry and then ball-milled in acetone for 10-15 hrs. The resulting slurry was air dried and then fired in a platinum dish at 1000-1300°C for 24 hrs. The growth furnace was R.F. induction heated and the crystals were grown by the Czochralski technique. The crystal growth procedure for the bronze crystals has been discussed in our earlier reports.

Since all of the compositions selected in this investigation are typically solid solution systems, single crystal growth by the Czochralski technique was found to be difficult, particularly for the K^+- and N^+-containing bronze compositions. The growth problems can be briefly summarized as follows:

1. Solid solution systems: difficult to determine the true congruent melting composition, hence optical striation problems.

2. Container contamination, specifically when an iridium cricible is used (inclusion of IrO_2 in grown crystals).

3. Cracking of crystals when cycling through the paraelectric/ ferroelectric phase transition temperature. This transition is often accompanied by a structural transition.

4. Exchange of crystallographic sites, e.g., for 15- and 12-fold coordinated sites under different growth conditions; hence difficult to maintain reproducible results.

In spite of these difficulties, several bronze composition crystals, e.g., KLN, BSKNN and PBN, have been successfully grown. Their growth problems and ferroelectric properties are discussed in this report.

2.2.2 Growth of KLN Crystals

$K_3Li_3Nb_5O_{15}$ (KLN) is tetragonal at room temperature with a point group 4 mm, and is typical of a completely filled tungsten bronze ferroelectric structure. It is well known that filled tungsten bronze compounds have high immunity to intense laser radiation damage and also exhibit interesting ferroelectric properties.

The KLN solid solution exists on the ternary phase diagram K_2O-Li_2O-Nb_2O_5 and, as shown in Fig. 2, this solid solution extends over a wide compositional range. The phase relation in this system has been studied by several workers[3,4] and, based on these investigations, it is clear that KLN single crystals with varying K:Li:Nb ratios can be grown. ("KLN" is the generally referred to name for the tungsten bronze solid solution within the compositional range shown in Fig. 2.) The Curie tempertaure shifts from 540° to 326°

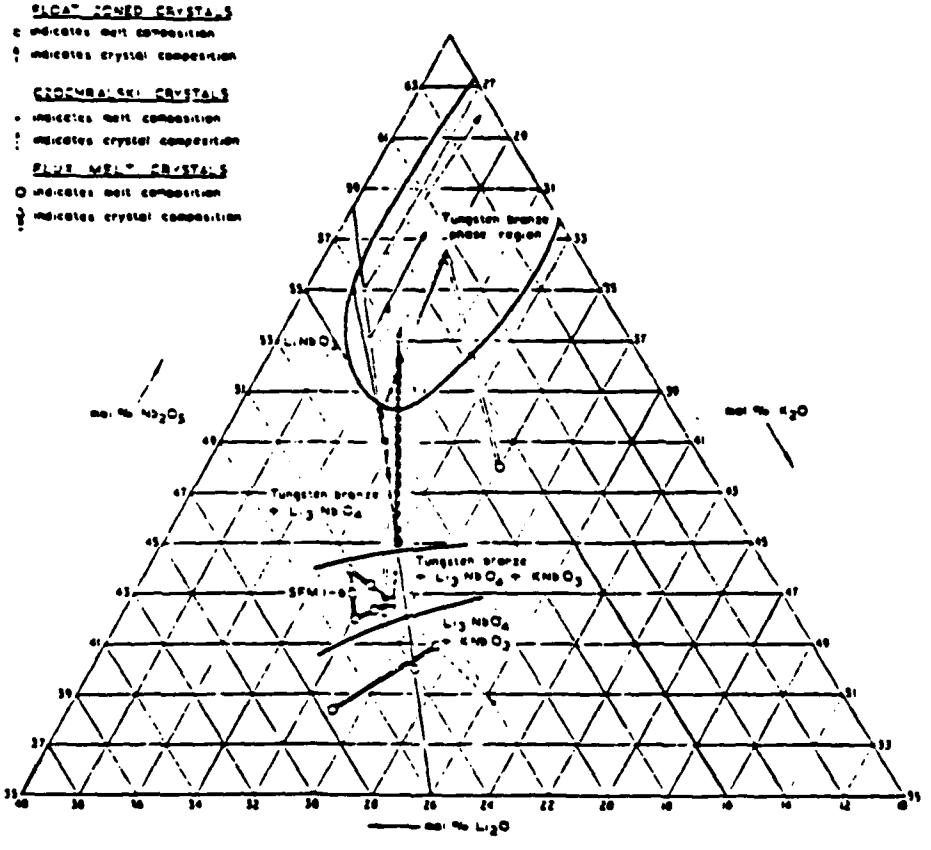

Fig. 2 Partial diagram of Li_2O-K_2O-Nb_2O_5 system in the region of the tungsten bronze field.

as the Nb_2O_5 concentration changes from 0.50 to 0.55. Recently, Adachi et al.[1] studied the single crystal growth of the composition $K_{2.89}Li_{1.55}Nb_{5.11}O_{15}$ and reported the successful growth of this composition (8-10 mm in diameter). These crystals showed excellent piezoelastic properties. Since this result seemed to be promising for this work, the composition $K_{2.89}Li_{1.55}Nb_{5.11}O_{15}$ was

chosen, and single crystals have been grown by the Czochralski technique from both iridium and platinum crucibles with successful results. For iridium crucibles, argon pressure had to be used to prevent loss of iridium, and as-grown crystals were found to be purple or coal black in color. However, the color changed to deep yellow when the crystals were subsequently annealed in oxygen above 800°C. Very low oxygen pressure was directly used when the platinum crucible was used as a container for crystal growth; crystals thus obtained were pale yellow in color. Since the lattice mismatch between $Sr_{0.60}Ba_{0.4}Nb_2O_6$ (SBN) (a = 12.47Å and c = 3.947Å) and KLN bronze compositions is minimal, SBN single crystals were used in the initial growth experiments as seed material. After achieving reasonable size KLN crystals, the KLN crystal itself was used as seed material in the subsequent experiments. This proved to be very successful, and crack-free KLN single crystals as large as 5-10 mm in diameter and 30-40 mm long have been successfully grown along the (100) direction (Table 3). Figures 3-5 show typical crystals grown along the (100) and (001) directions. In the course of this study, it was clearly observed that the rate of crystallization along the c-axis was much faster than for any other direction; the crystals, however, cracked when grown along the c-axis. This cracking problem was essentially eliminated when the crystals were grown along the a-axis, and such crystals are of excellent quality. Optimum growth conditions were found to be as follows:

Pulling Rate:	2-3 mm/hr
Rotation Rate:	20-30 rpm
Growth Direction	Along the a-axis
Growth temperature:	1000°C

The single crystal growth of KLN compositions has also been studied and reported by various other workers[3-12] and the results of this investigation are in close agreement with their findings. Although the KLN crystals obtained in the present work have been sufficiently large to initiate characterization studies, we have done considerable additional work on the

Table 3

Growth Conditions for Tungsten Bronze $K_3Li_2Nb_5O_{15}$ Single Crystals

Composition	Diameter of Crystal	Growth Direction	Crystal Quality	Curie Temp (°C)	Dielectric Constant K_{33}	Lattice Constant a_A	c_A
$K_3Li_2Nb_5O_{15}$	8-9 mm	(100)	Excellent	408	105	12.585	4.015
$K_3Li_2Nb_5O_{15}$	10-11 mm	(100)	Few Cracks	408	105	12.585	4.015
$K_3Li_2Nb_5O_{15}$	2-4 mm	(001)	Excellent	408	550	12.585	4.015
$K_3Li_2Nb_5O_{15}$	5-6 mm	(001)	Cracked	---	---	12.585	4.015
$K_3Li_2Nb_5O_{15}$	5-7 mm	(110)	Excellent	408	---	12.585	4.015

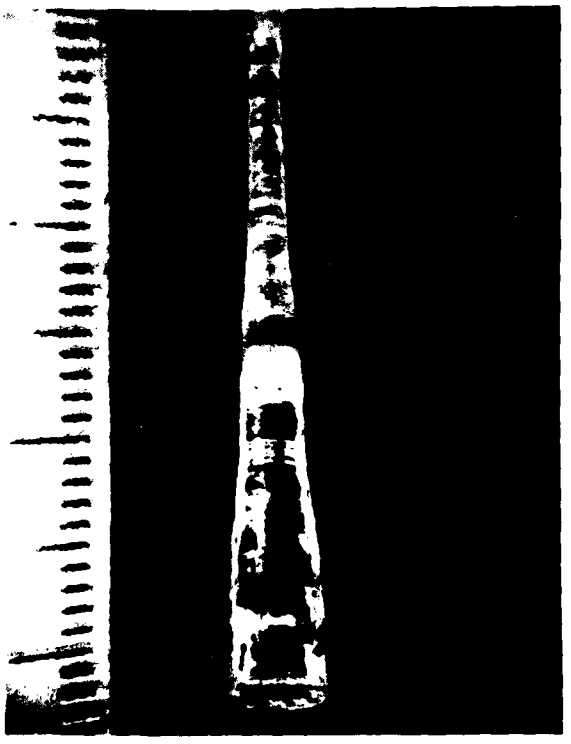

Fig 3
$K_3Li_2Nb_5O_2$ single crystal grown along the [100] direction, 6-7 mm in diameter.

Fig. 4
$K_3Li_2Nb_5O_{15}$ single crystal grown along the [100] direction, 10-11 mm diameter.

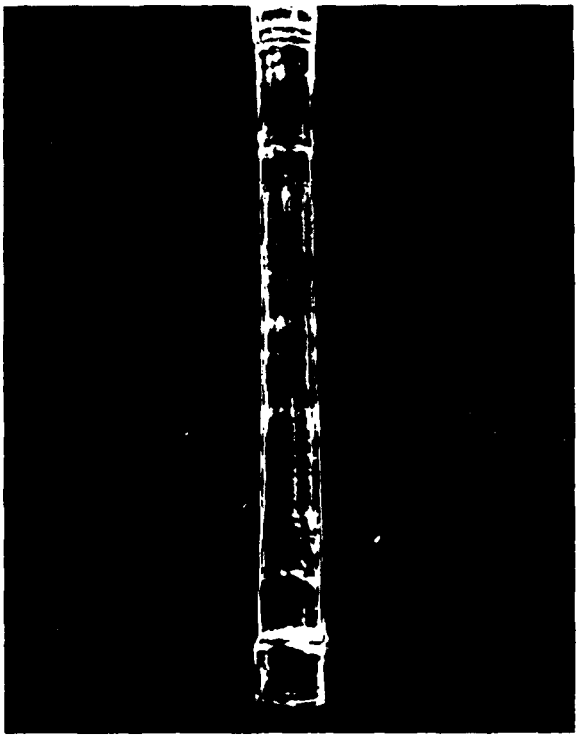

Fig. 5
$K_3Li_2Nb_5O_{15}$ single crystal grown along the [100] direction, 3 mm in diameter.

Czochralski growth technique in an attempt to obtain larger diameter, crack-free crystals. Based on our on-going research work on tungsten bronze family single crystals, it has been found that the growth of large-sized crystals depends strongly on the ability to control the diameter of the crystal and the thermal gradient in the crystal near the solid-liquid interface. However, in the case of KLN, we have not been able to grow crystals of > 1 cm diameter without considerable cracking.

2.2.3 Growth of BSKNN Crystals

Barium potassium niobate, $Ba_2KNb_5O_{15}$, is a well known ferroelectric tetragonal bronze composition and has been considered to be useful for high frequency and electro-optic studies. However, this composition has received very little attention since it melts incongruently. Our recent work on this system shows that the addition of Sr^{2+} for Ba^{2+} and Na^+ for K^+ as $Ba_{2-x}Sr_xK_{1-y}Na_yNb_5O_{15}$ (BSKNN) not only changes the congruency situation (compositions of interest are congruent melting), but also improves the dielectric, piezoelectric and electro-optic properties of this solid solution system. Although BSKNN is not considered to be a completely filled tungsten bronze like KLN, the 15- and 12-fold coordinated sites in this compositions are considered to be filled.

Recently, we studied the phase equilibria relation for this solid solution system and found that the compositions close to the $Ba_{1.2}Sr_{0.8}K_{0.75}Na_{0.25}Nb_5O_{15}$ region are congruent melting and appeared to be suitable for the proposed research work. Although the growth of several different composition crystals from this system with varying x and y have been planned, the work in this report is confined to the growth of $Ba_{1.2}Sr_{0.8}K_{0.75}Na_{0.25}Nb_5O_{15}$ (BSKNN) crystals.

Single crystals of BSKNN have been grown by the Czochralski technique from a platinum crucible. Although the lattice match between the bronze crystals SBN and BSKNN is not close, SBN crystals were used initially as seed material for the growth of BSKNN crystals. This proved to be successful in growing small crystals of BSKNN which were then used as seed material in subsequent

experiments to grow bigger and better quality crystals. BSKNN single crystals as large as 0.7 to 1.1 cm in diameter and 3-4 cm long have now been grown. Current growth parameters are as follows:

Pulling Rate:	6-8 mm/hr
Rotation Rate:	5 rpm
Growth Direction:	Along the c-axis
Growth Temperature:	1480°C

All of the $Ba_{1.2}Sr_{0.8}K_{0.75}Na_{0.25}Nb_5O_{15}$ crystals to date have been grown using a platinum crucible with an oxygen atmosphere. The resulting crystals are optically transparent and essentially colorless in appearance.

Crystals grown along the c-axis are usually faceted, which is quite exceptional for Czochralski-grown crystals. Figure 6 shows a typical crystal grown along the c-axis. In the course of this study, it was clearly observed that the rate of crystallization along the c-axis was greater than those along other directions (100, 110, etc.).

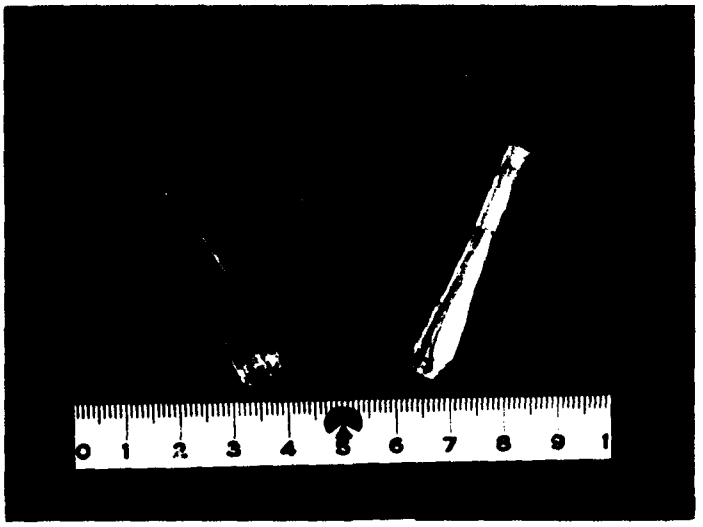

Fig. 6 Shows a typical 1 cm in diameter BSKNN single crystal grown along the C-axis.

2.2.4 Growth of $Pb_{1-x}Ba_xNb_2O_6$ Compositions

Compositions in the $Pb_{1-x}Ba_xNb_2O_6$ system belong to the tungsten bronze family and exhibit both orthorhombic and tetragonal structures as a function of Ba^{2+} concentration. Figure 7 shows the phase boundary conditions for these two phases. It can be seen that the substitution of Ba^{2+} for Pb^{2+} first decreases the orthorhombic distortion, and then induces a tetragonal structure at $x = 0.37$, with the polar axis along c-axis rather than along the orthorhombic b-axis. The second phase is tetragonal both above and below the ferroelectric Curie temperature, with a largely discontinuity in cell parameters at the Curie temperature. The substitution of Ba^{2+} in $PbNb_2O_6$ also causes remarkable changes in the ferroelectric properties, specifically at the morphotropic phase boundary ($x = 0.37$). The dielectric, electro-optic, piezoelectric, electromechanical and other ferroelectric properties are exceptionally large as one approaches this morphotropic phase boundary (MPB) region, and this offers an excellent opportunity to develop suitable materials from this system not only for SAW applications, but for several other potential applications including optical signal processing and pyroelectric thermal detectors.

Table 4 summarizes the ferroelectric structural properties for the $Pb_{1-x}Ba_xNb_2O_6$ system compositions. All of these compositions look promising; however, compositions close to MPB region have been selected in this work to study their SAW and optical properties. Although the compositions in this system melt congruently, bulk single crystal growth is difficult for the following reasons:

- Excessive loss of Pb^{2+} by evaporation, specifically for Pb^{2+}-rich compositions.
- Cracking of crystals when cycling through the ferroelectric/paraelectric phase transition. This transition is often accompanied by a structural transition.
- Reduction of Pb^{2+} to metallic lead to form a Pb-Pt alloy when inert or reducing conditions are used for growth.

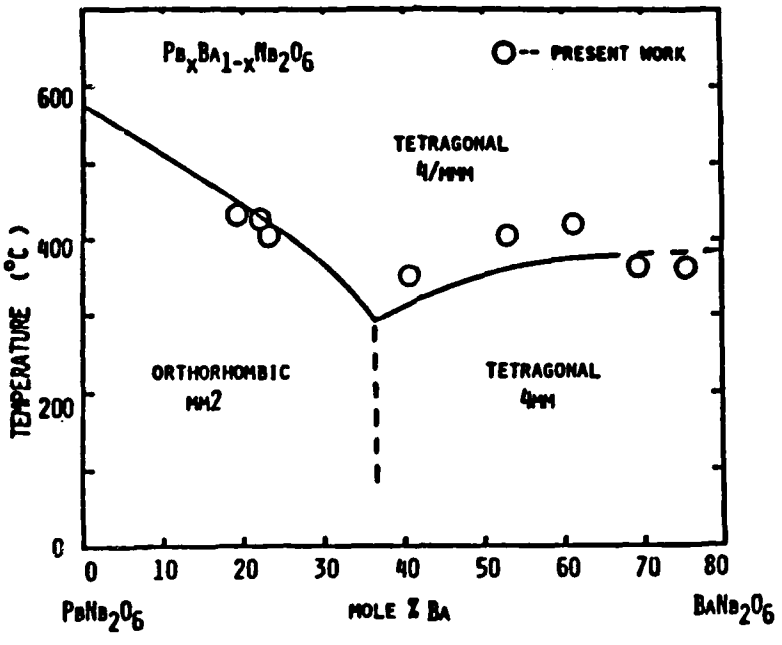

Fig. 7 Phase diagram for ferroelectricity in the solid solution system $Pb_{1-x}Ba_xNb_2O_6$.

Recently we developed the ternary phase diagram PbO-BaO-Nb_2O_5 (Fig. 8) and found that the stoichiometric compounds exhibit better properties as compared to lead-rich or lead-deficient compositions. However, the stoichiometric compounds were extremely difficult to prepare since control over lead losses was a major problem. However, it was also found that these lead losses were considerably suppressed when La^{3+} was added to these compositions. In our IR&D program, the hot pressing technique has been established for La^{3+}-doped and undoped compositions and found that these dense grain oriented samples are very promising for several applications. Samples as large as 1 to 2 in. in diameter have been hot-pressed successfully and these samples have been used for ferroelectric characterization. The compositions of the hot-pressed samples are as follows:

- $Pb_{0.60}Ba_{0.40}Nb_2O_6$, tetragonal (close to MBP condition)
- $Pb_{0.60}Ba_{0.4}Nb_2O_6:La^{3+}$, La^{3+} = 2, 4, 8 mole%.

Table 4

Properties of $Pb_{1-x}Ba_xNb_2O_6$ and Other Bronze Crystals

Composition	Melting Temperature (°C)	T_c (°C)	Lattice Parameters a_A°	b_A°	c_A°	Dielectric Constants k_a	k_b	k_c
$Pb_{0.30}Ba_{0.70}Nb_2O_6$	1380	350	12.450		3.995	340	-	95
$Pb_{0.27}Ba_{0.73}Nb_2O_6$	1380	350	12.500		2.975	360	-	140
$Pb_{0.48}Ba_{0.52}Nb_2O_6$	1360	407	12.493		3.987	-	-	-
$Pb_{0.60}Ba_{0.40}Nb_2O_6$	1350	345	12.495		3.990	1600	-	200
$Pb_{0.87}Ba_{0.13}Nb_2O_6$*	1350	430	17.670	17.92	3.890	1200	225	1900
$Ba_{2-x}Sr_xK_{1-y}Na_yNb_5O_{15}$	1480	203	12.506	-	3.982	450	-	250
$Sr_{0.5}Ba_{0.5}Nb_2O_6$	1520	125	12.483	-	3.956	-		500

*Orthorhombic bronze composition.

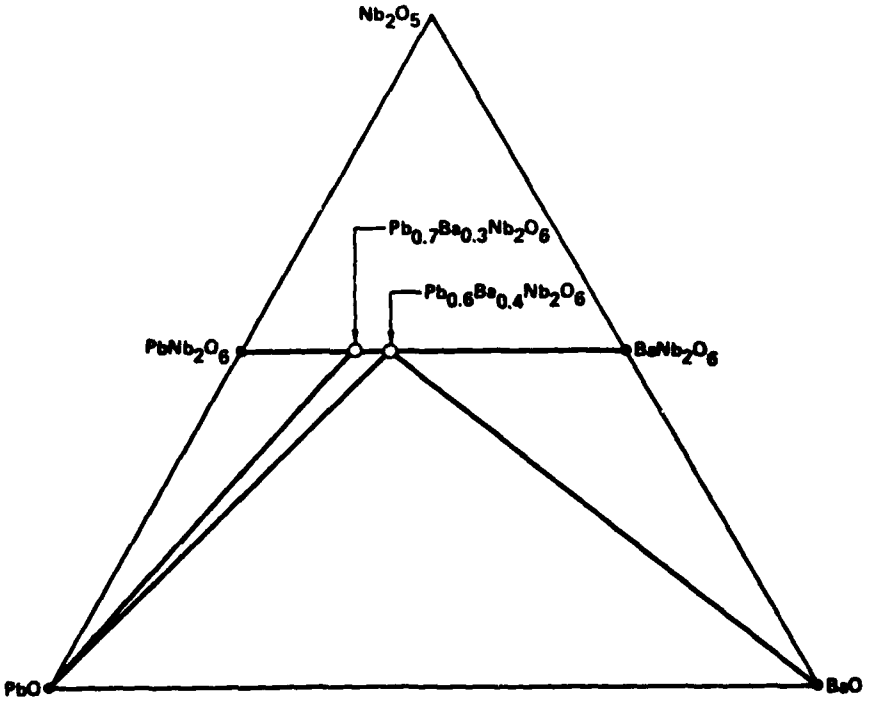

Fig. 8 PbO-BaO-Nb_2O_5.

It was found that the fabrication of orthorhombic $Pb_{1-x}Ba_xNb_2O_6$ was more difficult since samples cracked while cycling through the orthorhombic/tetragonal phase transition temperature. Because of these difficulties, the work in the present research was confined to only the tetragonal $Pb_{1-x}Ba_xNb_2O_6$ compositions.

At Penn State University (under DARPA Sponsorship), the growth of these compositions has been attempted using the Czochralski technique to develop small size crystals for SAW applications. Since the loss of Pb^{2+} is a severe problem in this system, the work at present has concentrated on the Ba^{2+} rich compositions, typically $Pb_{0.3}Ba_{0.7}Nb_2O_6$. The growth of 1 cm diameter crystals has been possible, but the crystals have cracked somewhat when cycling through the phase transition. However, crystals recovered in this growth are sufficiently large to study their ferroelectric, acoustical and electro-optic properties. Efforts are underway at Penn State as well as in our own laboratory to establish the growth technique for this composition and another important composition, $Pb_{0.6}Ba_{0.4}Nb_2O_6$. It is expected that the addition of La^{3+} or other dopants might reduce Pb^{2+} losses in these compositions.

The lattice constants for these compositions, as given in Table 4, are close to those for tetragonal BSKNN crystals; hence one would expect that these crystals should grow square with four well-defined facets. Since the Czochralski technique has not yet been fully established for these compositions, it is very difficult to state the growth habit for this particular system. Over the last several years, we have grown a number of bronze crystals and it has been shown that the existence of facets depends strongly on the thermal gradient near the solid-liquid interface. Once this problem is resolved for these compositions, it will be possible to establish the growth habit and other characteristics in detail. The current growth results (hot-pressing and crystal growth) are promising and we intend to continue this work for future electro-optic and pyroelectric research.

3.0 FERROELECTRIC PROPERTIES OF TUNGSTEN BRONZE CRYSTALS

Several techniques have been utilized to fully characterize the tungsten bronze single crystals and using such diverse techniques, it has been possible to optimize materials characteristics and performance for a given device application. The physical properties of these materials have now been established as a function of growth parameters.

3.1 Growth Habit and Structural Characteristics

As discussed in an earlier section, several bronze composition crystals, e.g., KLN, BSKNN, PBN have been grown successfully by the Czochralski technique. The results of this study indicate that the growth of K^+ and Na^+-conaining bronze crystals is difficult, and crystal size has been restricted to approximately 1 cm in diameter and 2 cm long. The crystals grown are fracture-free and are of good quality for SAW device studies. Although the growth of 1 cm diameter crystals is possible in the present set-up, the technique is confined to small size crystals basically due to a lack of complete understanding of these compositions. The phase diagram work on these systems needs to be studied further in order to establish the true congruent melting compositions in these systems. The crystals are usually colorless or pale yellow. KLN and BSKNN crystals grown along the c-axis are square and exhibit four well-defined facets (100). It is interesting to note that smaller crystals such as $Sr_{1-x}Ba_xNb_2O_6$ (SBN) or $Sr_2KNb_5O_{15}$ (SKN) have cylindrical growth habits and exhibit 24 well-defined facets. Figure 9 shows the growth habit for these smaller and bigger unit cell bronze crystals.

Structural analysis by the x-ray diffraction technique for ceramic and single crystals reveals that both powder and crystal forms show a room temperature tetragonal tungsten bronze structure and, according to the structural refinements, possess 4 mm point symmetry.

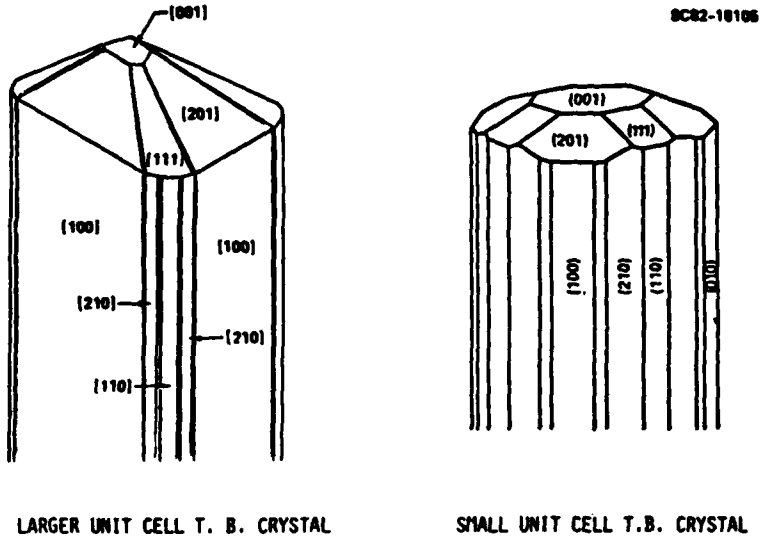

Fig. 9 Crystallographic features of small and large unit cell tungsten bronze crystals.

3.2 Ferroelectric Characteristics

3.2.1 Sample Preparation

Because of the large number of parameters needed to fully characterize the tetragonal (4 mm) bronze crystals, which include two dielectric, three piezoelectric and six elastic constants, several specimens with various shapes and orientations were used in the present investigation. Figure 10 shows the shapes and orientations of the crystals used for characterization. Prior to all ferroelectric measurements, the crystals were poled by the field-cooling method under a dc field of 5 to 10 kV/cm along the (001) direction. The temperature-time conditions for poling changes slightly when going from one bronze crystal composition to another. However, in general the bronze crystals were found to be relatively easy to pole as compared to perovskite crystals such as $BaTiO_3$ and $PbTiO_3$.

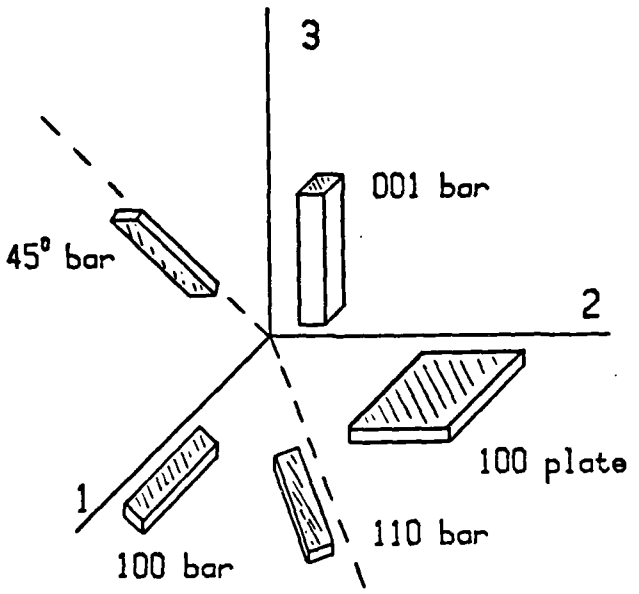

Fig. 10 Shapes and orientations of specimens.

The procedure for determining the elastic piezoelectric constants were similar to those described by Berlincourt and Jaffe in the case of $BaTiO_3$ utilizing the resonance-antiresonance transmission method. The dielectric constants were measured on (001) and (100) plates at 1 kHz, 100 kHz and 1 MHz using a Hewlett Packard 4270A automatic capacitance bridge. The spontaneous polarization (P_s) as function of temperature was determined statically. An electrically poled sample being equilibriated at some temperature T ($T < T_c$) was thermally depoled by quenching in a 200°C silicone oil bath while the charge was collected using an electrometer.

3.2.2 Dielectric Properties

Table 5 summarizes the results of several measurements, including structural, dielectric, ferroelectric and electro-optic, for KLN, BSKNN, PBN

Table 5

Important Piezoelectric Properties of Tungsten Family Crystals

Property	$Pb_2KNb_5O_{15}$ (PKN)	$Ba_2NaNb_5O_{15}$ (BNN)	$Sr_{0.6}Ba_{0.4}Nb_2O_6$ (SBN)	$K_3Li_2Nb_5O_{15}$ (KLN)	$Ba_{2-x}Sr_yK_{1-y}Na_yNb_5O_{15}$ (BSKNN)	$Pb_{0.3}Ba_{0.7}Nb_2O_6$ (PBN)
Electromechanical Coupling Constant k_{33}	---	0.45	0.45	0.52	k_{33} = 0.47	k_{33} = 0.52
k_{15}	0.69	0.12	0.24	0.34	k_{15} = 0.28	k_{15} = 0.25
k_{24}	0.73	0.25	---	---	---	k_{31} = 0.15
Piezoelectric Constant (10^{-12} C/N)	d_{33} = 62 d_{15} = 470 d_{24} = 470	d_{15} = 32 d_{24} = 45	d_{33} = 130 d_{15} = 31	d_{33} = 57 d_{15} = 68	d_{33} = 60 d_{15} = 70	d_{33} = 60 d_{15} = 50 d_{31} = 12
SAW-Electromechanical Coupling Constant (K^2)	188×10^{-4}	---	180×10^{-4}	---	---	---
Temperature Coefficient of SAW Velocity	Y-cut,+24 ppm Z-cut,-30 ppm	Close to α-quartz	Z-cut,-50 ppm (110),-18 ppm	---	---	---
Curie Temperature (°C)	460	560	72	405	203	---
Crystal Symmetry	Ortho T.B.	Ortho T.B.	Tetra T.B.	Tetra T.B.	Tetra T.B.	Tetra T.B.
Dielectric Constant @ 23°C		ε_{33} = 43 ε_{11} = 248	ε_{33} = 880 ε_{11} = 450	ε_{33} = 100 ε_{11} = 309	ε_{33} = 250 ε_{11} = 450	ε_{33} = 95 ε_{11} = 340
Electro-optic Coefficient $\times 10^{-12}$ m/V	---	r_{51} = 95 r_{33} = 30 r_{42} = 80	r_{33} = 420 r_{13} = 40 r_{52} = 80	r_{33} = 80 r_{13} = 10	r_{33} = 360	
Pyroelectric Coefficient 10^{-12} C/N	---	420	850	---	440	170

and also for PKN, BNN and SBN crystals. The temperature dependence of the dielectric constants ε_{33} and ε_{11} (zero stress) and loss ($\tan\delta$) were determined from poled and unpoled plates for all of the crystals listed in Table 5. Figures 11 and 12 show the temperature dependence of the dielectric constant for BSKNN. These measurements were made from room temperature up to 600°C with nominal heating and cooling rates of 2-4°C/min. Both ε_{33}, and to a lesser extent ε_{11}, showed marked anomalies at the Curie transition at 203°C. The general temperature behavior and large anisotropy of ε_{33} and ε_{11} are typical of most tetragonal ferroelectric bronzes. However, the magnitude of the dielectric constant at a given temperature is markedly different for each composition, and seems to strongly depend on the size of the unit cell of the

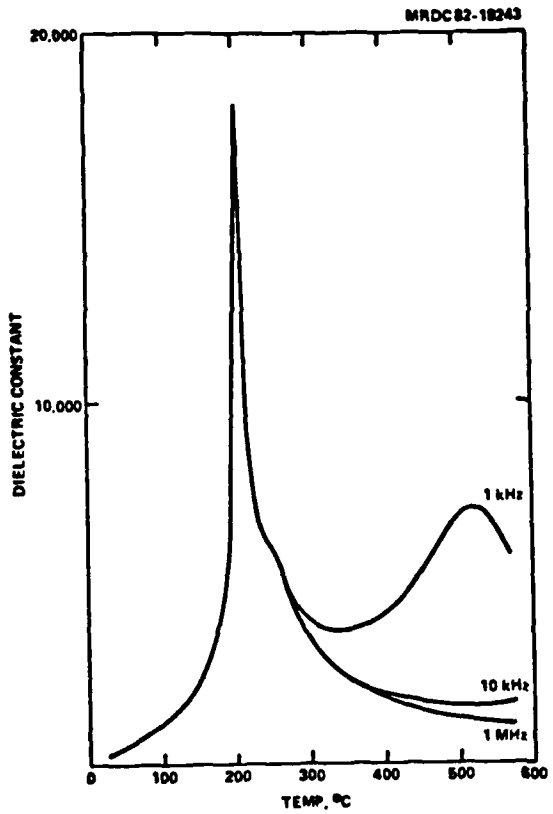

Fig. 11
Dielectric constant vs temperature for $Ba_{0.2}Sr_{0.8}K_{0.75}Na_{0.25}Nb_5O_{15}$ single crystal, measured along [001] axis.

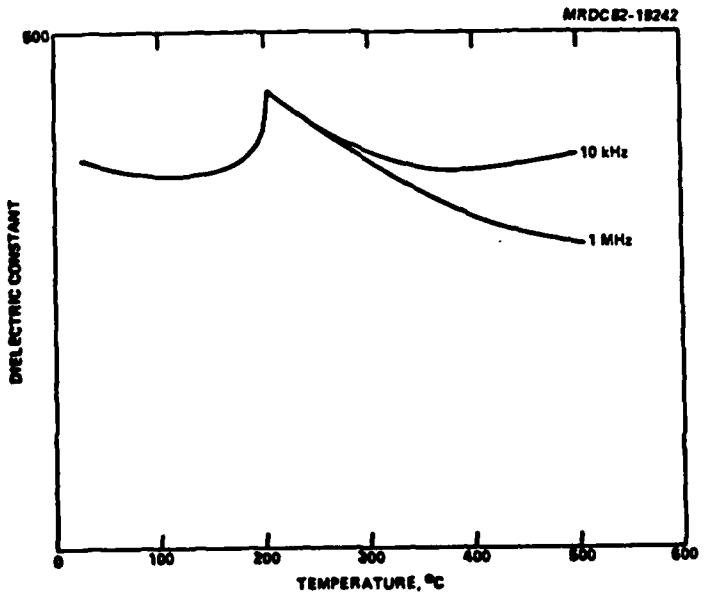

Fig. 12 Dielectric constant vs temperature for $Ba_{0.2}Sr_{0.8}K_{0.75}Na_{0.25}Nb_5O_{15}$ single crystal, measured along [100] axis.

particular bronze crystal. For example, at room temperature ε_{33} is large while ε_{11} small for the smaller unit cell bronzes, e.g., $Sr_{1-x}Ba_xNb_2O_6$ (SBN) and $Sr_2KNb_5O_{15}$ (SKN), primarily as a result of the relatively low Curie temperature for these bronzes. On the other hand, the situation is reversed in the case of the bigger unit cell bronzes where ε_{33} is smaller than ε_{11} at room temperature, as in the present case of BSKNN. The dielectric losses ($\tan\delta$) at room temperature over the frequency range of 100 Hz-1 MHz are on the order of 0.05 or less for the c-axis, and 0.01 or less for the a and b axes of material which has not been poled. With poling, the c-axis losses and ε_{33} decrease, whereas ε and $\tan\delta$ remain essentially unchanged for the a and b axes.

The dielectric properties were further studied by cooling below room temperature, and it was found that in case of bigger unit cell bronzes the dielectric constant ε_{11} gradually increases with decreasing temperature, indicating the existence of another ferroelectric-ferrolectric or ferroelectric-ferroelastic phase transition. This type of behavior has also been noted for another bronze composition, $Ba_2NaNb_5O_{15}$, and other ferroelectric families including perovskite ($BaTiO_3$, PZT, KTN, etc.), KDP, and others. Further work is in progress on BSKNN, KLN and PBN crystals to establish the existence of a low temperature transition and the ferroelectric properties below room temperature.

The electromechanical coupling, piezoelectric, electro-optic and pyroelectric coefficients for the bronze crystals are summarized in Table 5. It can be seen that the piezoelectric coefficients are different for bigger and smaller unit cell bronzes. For example, d_{15} is large while d_{33} is smaller for the BSKNN, KLN and PBN compositions. On the other hand, the piezoelectric d_{33} coefficient is large while d_{15} is smaller for smaller unit cell bronzes, e.g., SBN and SKN. Similarly, although k_{15} is smaller than k_{33} for all bronzes, the value of this coefficient is generally larger for the bigger unit cell bronzes. However, other properties such as the electro-optic and pyroelectric coefficients are large for all bronzes and appear to be less affected

when going from smaller to bigger unit cell bronze crystals. These results are interesting, and further work is in progress to examine the correlation of these characteristics with the piezoelectric and dielectric properties. At the present time, PBN, BSKNN, SBN and PKN crystals appear to be more interesting for SAW device studies and work should continue in that direction. Table 6 summarizes the classification of tungsten bronze crystals based on their unit cell dimensions, growth habit and ferroelectric properties. It is expected that this classification will be found useful for the selection of proper bronze compositions for new device applications.

Table 6

Classification of Tungsten Bronze Family

T.B. Compositions with Smaller Unit Cell Dimensions	T.B. Compositions with Larger Unit Cell Dimensions
e.g., $Sr_{1-x}Ba_xNb_2O_6$ $Sr_2KNb_5O_{15}$ $Sr_2NaNb_5O_{15}$	e.g., $Ba_6Ti_2Nb_8O_{30}$, $Sr_2Ti_2Nb_8O_{30}$ $Ba_{2-x}Sr_xKNb_5O_{15}$, etc.
• Crystal habit is cylindrical with 24 well-defined facets	• Crystal habit square with 4 well-defined facets
• High electro-optic and pyroelectric effects	• High electro-optic coefficient
• High delectric constant	• Relatively low dielectric constant
• High piezoelectric d_{33} coefficient but low d_{15}	• High piezoelectric d_{15} coefficient, but low d_{33}
• Large crystals with excellent quality are available (2-3.0 cm in diameter)	• Moderately large crystals are available (~ 1-1.5 cm)
• Low phase transition temperature (below 200°C)	• High phase transition temperature (over 200°C)

3.2.3 Acoustical Characteristics

The acoustical properties of the tungsten bronze compositions are of significant interest from the device point of view, and this work should continue to establish suitable materials from this family. We believe that the current bronze compositions based on the KLN, BSKNN and PBN systems will satisfy current needs. Recently we successfully demonstrated the usefulness of tungsten bronze SBN:60 and SBN:50 crystals for acoustical device studies. Table 7 summarizes the acoustical characteristics for these crystals studied under DARPA contract. The electromechanical coupling constants (K^2) for the (100), (110) and (001) orientations of SBN:60 and SBN:50 bulk crystals has been established. These constants have been shown to be substantially larger for the (001)-plate propagating along the (100) direction with a value of 230×10^{-4}. This value is smaller than the best known piezoelectric Y-Z cut $LiNbO_3$ crystal (480×10^{-4}), but it is similar to the best known piezoelectric tungsten bronze, $Pb_2KNb_5O_{15}$ (188×10^{-4}). Measurements on (100) and (110) plates propagating (001) directions show large coefficients, but they are lower than for the (001) plate. The temperature coefficient of SAW velocity for the three different cuts are also given in Table 7.

Both PKN and SBN crystals now appear to be important materials for SAW device studies; however, PKN crystals are not available due to the extreme difficulty in obtaining good quality crystals of sufficient size. PKN crystals often crack (practically shatter) while cycling through the paraelectric/ferroelectric phase transition temperature, thus rendering them useless for any device studies. On the other hand, the growth of tetragonal tungsten bronze crystals has been shown to be more feasible, and crystals such as SBN:60, SBN:50, KLN, BSKNN and PBN of suitable size and quality have been grown in this study and in other programs. The acoustical characteristics of SBN:60 and SBN:50 crystals are generally comparable to those of PKN. It has been shown that the physical properties of significance for SAW applications are the electromechanical coupling and piezoelectric coefficients and the dielectric constants. All of these properties have been shown to be better

Table 7

Acoustical Characteristics of the SBN:60 and SBN:50 Single Crystals

Crystal Composition	SAW-Electromechanical Coupling Constant (K^2)	SAW-Velocity m/s	Temp. Coef. of SAW-Velocity, at Room Temperature
SBN:60-(001) Plate Propagating along the [100] direction	180×10^{-4}	3300	-50 to -140 ppm/°C
SBN:60-(100) Plate Propagating along the [001] direction	55×10^{-4}	3193	
SBN:60-(100) Plate	60×10^{-4}	3173	-18 ppm
SBN:50-(001) Plate Propagating along the [100] direction	230×10^{-4}	3270	-33 ppm/°C
SBN:50-(110) Plate Propagating along the [001] direction	30×10^{-4}	3120	-17 ppm/°C

for KLN, BSKNN and PBN, making these crystals potentially important for the future acoustical work. It is expected that the continuation of present work on these tungsten bronze crystals should result in the production of interesting and suitable compositions for SAW and other device applications.

4.0 SUMMARY AND RECOMMENDATION

During the course of this investigation over the past three years, we have successfully demonstrated the growth of good quality and crack-free medium size tungsten bronze crystals of various compositions including KLN, BSKNN, and PBN, by the Czochralski technique. Although further improvements are necessary in the current growth technique, specifically for the PBN system crystals, these crystals have created new interest in this family for various applications which include SAW, electro-optic, pyroelectric, photorefractive and millimeter wave, as summarized in Table 8.

Table 8
Applications of T.B. Crystals

Applications	Key Characteristics*	Device
SAW	• Large d_{15}, d_{33}, k_{33}, ε_{33} • Temperature compensated orientations	
Thermal Detector (Pyroelectric)	• Large pyroelectric coef. • Low dielectric loss ($\tan\delta$)	• Vidicon and focal plane arrays
Optical (Electro-optic)	• Large r_{33}, r_{52} • Photorefractive sensitivity and speed • Structure flexibility for doping	• Modulator and wave guides • Holographic storage and optical signal processing • SLM and filters
High Frequency	• Large dn/dE • Low $\tan\delta$ (0.03) • Complete transmission	• Millimeter wave shifter • Optical modulators • Frequency doubler

*All of these characteristics are large and adjustable with device needs.

The main objective of the present research has been to investigate the SAW properties of these bronze crystals and examine their applicability for device usage. The results of this study indicate that the piezoelectric properties of the bigger unit cell bronzes are superior since d_{15}, d_{33}, k_{15}, k_{33}, and the dielectric constants are quite different from the smaller unit cell bronzes, with resultant lower acoustical losses. Although all of the acoustical characteristics of the bigger unit cell bronzes are not yet known, it is expected that crystals from the PBN system should prove to be important for SAW device studies. As reported in earlier sections, both PKN and SBN are also useful for SAW applications. However, it must be stated that in the case of SBN crystals the ferroelectric phase transition temperature is quite low, and this may be a problem for device applications. On the other hand, all of the bigger unit cell bronzes have their phase temperature over 200°C, and can therefore be easily processed. This is an unique advantage for these materials and appears to be important for any future device study considerations. Furthermore, the excellent lattice match of these crystals to a number of other bronze compositions also make BSKNN and PBN potentially useful as substrate materials for liquid phase epitaxial (LPE) growth of bronze composition thin films.

We are continuing our efforts in the growth and characterization of large diameter, crack-free single crystals of PBN and BSKNN, and anticipate that both of these bronze compositions will find interest in a number of device applications as outlined in Table 8. It should be noted that the application of these crystals is suggested based on the figures of merit in each case. For future work, we offer the following recommendations:

- Establish the phase relation work for the BSKNN and PBN systems to establish true melting compositions. This will allow the growth of better quality and larger size crystals.

- Establish the low temperature ferroelectric properties of the bigger unit cell bronzes, so that one can correlate the significance of higher piezoelectric properties for these bronze compositions.

- Establish the acoustical properties of these bronzes with respect to low and high frequencies.

- Establish the electro-optic and pyroelectric properties of these crystals with respect to temperature.

5.0 PUBLICATIONS AND PRESENTATIONS

5.1 Publications

1. R.R. Neurgaonkar, W.K. Cory and J.R. Oliver, "Growth and Applications of Ferroelectric Tungsten Bronze Family Crystals," Ferroelectrics, 5 (1-4), 65, 1983.

2. R.R. Neurgaonkar, J.R. Oliver and W.K. Cory, "Single Crystal Growth and Piezoelectric Properties of Tungsten Bronze $Ba_{2-x}Sr_xK_{1-y}Na_yNb_5O_{15}$ Crystals," submitted to Mat. Res. Bull.

3. R.R. Neurgaonkar, J.R. Oliver and W.K. Cory, "Single Crystal Growth and Piezoelectric Properties of $K_3Li_2Nb_5O_{15}$ Crystals," to be submitted to J. Cryst. Growth.

5.2 Presentations

1. R.R. Neurgaonkar, W.K. Cory and J.R. Oliver, "Growth and Applications of Ferroelectric Tungsten Bronze Family Crystals," presented at IEEE Intl. Symposium on Applications of Ferroelectrics, Gaithersberg, MD, June 1-3, 1983.

2. R.R. Neurgaonkar, J.R. Oliver and L.E. Cross, "Growth and Applications of Ferroelectric Tungsten Bronze Family Crystals," presented at the 5th European Meeting on Ferroelectricity, Benalmadena, Spain, September 26-30, 1983.

6.0 REFERENCES

1. M. Adachi and A. Kawabata, "Elastic and Piezoelectric Properties of $K_3Li_2Nb_5O_{15}$ Crystals," Jap. J. Appl. Phys. 17, 1969 (1978).

2. R.R. Neurgaonkar, M.H. Kalisher, T.C. Lim, E.J. Staples and K.L. Keester, "Czochralski Single Crystal Growth of $Sr_{0.61}Ba_{0.39}Nb_2O_6$ for SAW Device Applications," Mat. Res. Bull. 15, 1235 (1980).

3. B.A. Scott, E.A. Giess, B.L. Olson, G. Burns, A.W. Smith and D.F.O. Kena, "The Tungsten Bronze Field in the System K_2O-Li_2O-Nb_2O_5," Mat. Res. Bull. 5, 47 (1970).

4. F.W. Ainger, J.A. Beswick, W.P. Bickley, R. Clarke and G.V. Smith, "Ferrolectrics in the Lithium Potassium Niobate System," Ferroelectrics 2, 183 (1971).

5. T. Yamada, "Elastic and Piezoelectric Properties of $PbKNb_5O_{15}$," J. Appl. Phys. 46, 2894 (1975).

6. Paul H. Carr, "New Temperature Compensated Materials for SAW Devices," Proceedings of IEEE Ultrasonic Symposium, 286, (1974).

7. T. Nagai and T. Ikeda, "Pyroelectric and Optical Properties of $K_3Li_2Nb_5O_{15}$," Jap. J. Appl. Phys. 12, 199 (1973).

8. T. Fukuda, "Growth and Crystallographic Characteristics of $K_3Li_2Nb_5O_{15}$ Single Crystals," Jap. J. Appl. Phys. 8, 122 (1969).

9. T. Fukuda, "Growth and Crysallographic Characteristics of $K_3Li_2Nb_5O_{15}$ Single Crystals," Jap. J. Appl. Phys. 9, 599 (1970).

10. T. Fukuda, H. Hirano and S. Koide, "Growth and Properties of Ferroelectric $K_3Li_2(Nb_{1-x}Ta_x)_5O_{15}$," J. Cryst. Growth 6, 293 (1970).

11. Y. Uematsu and S. Koide, "Piezoelectric Properties of Ferroelectric $K_3Li_2(Nb_{1-x}Ta_x)_5O_{15}$," Jap. J. Appl. Phys. 9, 336 (1970).

12. W.A. Bonner, W.H. Grodiewicz and L.V. Van Uitert, "The Growth of $K_3Li_2Nb_5O_{15}$ Crystals for Electro-Optic and Nonlinear Applications," J. Cryst. Growth 1, 318 (1967).

13. R.R. Neurgaonkar, "Temperature Compensated Piezoelectric Materials," Final Report, DARPA Contract No. F49620-78-C-0093 (1982).

14. E.A. Giess, G. Burns, D.F. O'Kane and A.W. Smith, "Ferroelectric and Optical Properties of $Sr_2KNb_5O_{15}$," Appl. Phys. Lett. 11, 233 (1967).

END

DATE
FILMED

7 - 84

DTIC